Relative Quantification of Deuterated Omega-3 and -6 Fatty Acids and Their Lipid Turnover in PC12 Cell Membranes Using ToF-SIMS

Mai H. Philipsen[1,3], Sanna Sämfors[1,3], Per Malmberg[1,3], and Andrew G. Ewing[1,2,3,*]

1. Department of Chemistry and Chemical Engineering, Chalmers University of Technology, Gothenburg 412 96, Sweden

2. Department of Chemistry and Molecular Biology, University of Gothenburg, Gothenburg 412 96, Sweden

3. Go:IMS, Chalmers University of Technology and University of Gothenburg, Gothenburg 412 96, Sweden

[*]To whom correspondence should be addressed

e-mail: andrew.ewing@chem.gu.se

Running title: ToF-SIMS for lipid turnover from omega-3 and -6 fatty acids

Abstract:

Understanding fatty acid metabolism and lipid synthesis requires a lot of information about which fatty acids and lipids are formed within the cells. In this study, we focused on the use of deuterated tracers of α-linolenic acid and linoleic acid to determine the relative amounts of their converted polyunsaturated fatty acids (PUFAs) and specific phospholipids incorporated into cell plasma membranes. Time-of-Flight Secondary Ion Mass Spectrometry (ToF-SIMS) was used to image and analyze lipids in model cell membranes with and without fatty acid treatment. Owing to the advantages of high mass and spatial resolution, ToF-SIMS can be used to simultaneously provide both chemical information and distribution of various molecules in the sample surface down to the subcellular scale. Data obtained from this analysis of isotopes in the cell samples have been used to calculate the relative amounts of long chain PUFAs and phospholipids from their precursors, α-linolenic acid and linoleic acid. Our results show that the fatty acid treatments induce an increase in amounts of α-linolenic acid and linoleic acid and their long chain conversion products. Moreover, an enhanced level of phospholipid turnover of these fatty acids, in lipids such as phosphatidylcholines, phosphatidylethanolamines, and phosphatidylinositols, is also observed in the cell plasma membrane.

Keywords: Mass spectrometry imaging, phospholipids, α-linolenic acid, linoleic acid, lipid turnover.

Introduction

The human body can metabolize all fatty acids (FAs) it requires except for two, α-linolenic acid (ALA, 18:3n-3) belonging to the omega-3 (n-3) family, and linoleic acid (LA, 18:2n-6) classified in being in the omega-6 (n-6) family. The FAs function as precursors for a series of n-3 and n-6 long chain polyunsaturated fatty acids (PUFAs) via a FA synthesis process of desaturation and elongation reactions (1). PUFAs have been shown to exhibit health benefits in various ways and are involved in immune, heart and brain function in addition to infant cognitive development (2). For example, ALA is converted into its metabolites, such as eicosapentaenoic acid (EPA, C20:5n-3) and docosahexaenoic (DHA, C22:6n-3) which are important in immune regulation, inflammatory processes and cognition (3). Additionally, arachidonic acid (AA, C20:4n-6), a lipid that is partly converted from LA, is a key mediator and regulator of inflammation (4). Lack of intake of these two PUFAs causes increased risk of diseases involving inflammatory processes such as obesity, cancer, and cardiovascular disease, as well as neurodegenerative illness (5, 6). Another study from Parletta *et al*. also showed that lower levels of DHA, EPA, and AA in human blood correlates with attention deficit hyperactivity disorder (ADHD) and autism (7).

Changes in PUFAs following ALA and LA supplements have been shown in preliminary studies to be useful in preventative treatment against neurodegenerative disease as well as cardiovascular disease (8-10). For example, n-3 PUFAs have been shown to be associated with prevention and treatment of dementia[9,] and ADHD (9, 11). Treatment with n-3 PUFA supplements that increase the n-3/n-6 PUFA ratio have been shown to reduce cognitive impairment in transgenic mice (12-14). The formation of new membranes induced by n-3 and n-6 FAs can influence the expansion of synaptic connections, which in turn can play an important role in neurotransmission (15, 16). Since the many roles of PUFAs in biological processes are starting to be revealed, a proper understanding of their converted acid and phospholipid turnover is needed. This is especially true regarding the contribution of PUFAs and their specific phospholipid turnover in prevention of age related disruption of brain function. Several studies have revealed changes in lipids containing long chain PUFAs after treatment with n-3 and n-6 FAs in rats and cells (17). However, the information about which specific phospholipids incorporate the fatty

acids remains unknown. An understanding about membrane lipid turnover and incorporation of PUFAs might provide a link between incorporation-specific lipids and mental illnesses.

Conventional mass spectrometry (MS) approaches can be used to identify levels of fatty acids and lipids in biological samples (18). MS provides quantification of lipids with low detection limit, high sensitivity, and wide dynamic range. Mass spectrometry imaging provides a tool that combines quantitative and qualitative information with spatial localization of molecules on the sample surface. The material on the surface is removed by either a laser or ion beam and is then analyzed. In contrast to conventional approaches, the cell or tissue samples are directly analyzed without a requirement for further sample preparation (19). In recent years, ToF-SIMS has become widely used for mass spectrometry imaging, applied in wide range of application fields, such as materials, clinical research, and biomedical analysis using a variety of different ion beams (Bi_n, C_{60}^+, Au_n) (19-21). Recently, the application of gas cluster ion beams (GCIB) as the analysis beam has shown great promise for analysis of lipids. GCIBs have shown signal improvement for analysis of intact lipid species with advantages including low surface damage and reduced fragmentation (22, 23).

In this paper, we took advantage of two types of ToF-SIMS instruments to obtain the chemical localization of biomolecules in cells: an *ION-TOF V* equipped with a 25 keV bismuth liquid metal ion gun (LMIG) and a *J105* ToF-SIMS equipped with a 40 keV CO_2 GCIB. Detection of deuterated species at the nanoscale with high spatial resolution was carried out with the LMIG, whereas the GCIB provided higher signals for higher mass species, such as intact lipids. The ability to combine good spatial resolution with high mass resolution and high mass molecular ion analysis provides more distribution-specific information of incorporated lipid species from n-3 and n-6 FAs on the cellular scale. We used stable isotopically labeled FAs to trace phospholipid synthesis and transport into the plasma membrane of PC12 cells with ToF-SIMS. Deuterated and nondeuterated fatty acids were used to incubate cells; then the relative amount of phospholipid turnover from FAs in the cellular membrane was determined based on the signals from the isotope peaks obtained from the ToF-SIMS spectra. Our data show an increase in the content of fatty acids and phospholipids in the plasma membrane. Isotope tracer studies

also indicated the incorporation of deuterated fatty acids into unsaturated phosphatidylcholines (PCs), phosphatidylethanolamines (PEs), and phosphatidylinisitols (PIs), and from this we show that the conversion PUFAs from both ALA and LA is different, and we suggest a pathway for lipids in protection against unhealthy brain aging.

Materials and Methods

Chemicals

[D5] α-linolenic acid ($^2H_5C_{18}H_{25}O_2$, MW 283.25) and [D2] linoleic acid ($^2H_2C_{18}H_{30}O_2$, MW 282.25) were purchased from Lipidox, Sweden. Non-deuterium-labeled α-linolenic acid (18:3n-3, $C_{18}H_{30}O_2$, MW 278.22 g/mol) and linoleic acid (18:2n-6, $C_{18}H_{30}O_2$, MW 280.24 g/mol) were obtained from Sigma-Aldrich, Germany.

Cell sample preparation

PC12 cells were donated by Lloyd Greene's lab (Columbia University, USA). The cells were maintained in RPMI-1640 media (PAA laboratories, Inc. Australia) supplemented with 10% donor equine serum (PAA laboratories) and 5% fetal bovine serum (PAA laboratories). The cells were plated in collagen coated flasks (Collagen type IV, BD Bioscience, Bedford, MA) and incubated in a 7% CO_2, 100% humidity environment at 37ºC. The cell medium was changed every 2 days and the cells were subcultured every 7 days.

For experiments, cells were grown on poly-ι-lysine coated silicon wafers for 3 days. Cells were incubated with RPMI-1640 media supplemented with 10% donor equine serum and 5% fetal bovine serum, containing 100 μM of deuterated or nondeuterated fatty acids (ALA and LA) for 1 day. The silicon wafers were then rinsed 3 times with ammonium formate (Sigma Aldrich) 50 mM, pH 7.4. After removing the excess liquid on the surface, the silicon wafers were fast-frozen in isopentane at -185ºC to avoid the formation of water crystals on the sample surface, and thereafter freeze-dried. The samples were introduced into the analysis chamber of the ToF-SIMS instruments for analysis. Two silicon wafer slides containing cells for each sample were prepared. The experiments were repeated with 3 cell

generations. Each generation was repeated twice.

ToF-SIMS imaging - *ION TOF V*

SIMS imaging was performed with an ION-TOF V (ION-TOF, GmbH, Germany) equipped with a 25 keV bismuth liquid metal cluster ion gun. The bunched mode with Bi_3^{++} primary ions gave a high mass resolution of m/Δm 7000 with a pulsed current of 0.3 pA. The primary ion dose density was 2 x 10^{12} ion/cm^2 in both positive and negative ion modes for an image area of 255 x 255 μm^2 with 256 x 256 pixels. A low energy electron flood gun was used to neutralize the charge on the sample surface.

ToF-SIMS analysis - *J105*

ToF-SIMS analysis was also performed using a *J105* ToF-SIMS instrument (Ionoptika Ltd, UK), that has been described in detail elsewhere (24, 25). The instrument was equipped with a quasi-continuous primary ion beam that was used to bombard the sample to produce a stream of secondary ions that were bunched to produce a tight packet of ions at the entrance of a reflectron ToF analyzer. In this study, a 40 keV GCIB was used. Clusters were formed by the expansion of CO_2 into a vacuum chamber and further ionized by electron impact. The GCIB improves the surface smoothness and minimizes subsurface chemical damage due to their low individual atomic interactions. A Wien filter was used to select a cluster size range of n = 6000 (approximately ±2000). Spectra were acquired over an 800 × 800 μm^2 area, at pixel resolution of 6.26 μm^2/pixel. The primary ion dose density for each image was approximately 1 × 10^{13} ions/cm^2. In the negative ion mode, low energy (12 eV) electron flooding was used to decrease the effects from sample charging. The instrument provided mass resolution of 10000 for *m/z* 772.6.

Data analysis

ToF-SIMS spectra and images obtained from the *ION-TOF V* were processed with Surface Lab software (version 6.3 ION-ToF, GmbH, Münster, Germany). The region of interest covered only cells and was selected to minimize the contribution from background signals around the cells. The spectra obtained were calibrated to the peaks at $[CH_3]^+$, $[C_2H_5]^+$, $[C_3H_7]^+$, and $[C_5H_{15}PNO_4]^+$ for positive ion mode; and $[CH]^-$, $[C_2]^-$, $[C_3]^-$, $[C_{18}H_{33}O_2]^-$ for negative ion mode.

TOF-SIMS data from the *J105* were processed using the Ionoptika Image Analyser 2D program developed by Ionoptika Ltd. Pixels containing cells were picked by imaging *m/z* 184.1 (PC fragment)

for positive ion mode and *m/z* 885.6 (PI(38:4)) for negative ion mode. Data were normalized to the number of pixels chosen in the region of interest. For positive ion mode, data were normalized to PC head group at *m/z* 184.1 and for negative ion mode, data were normalized to PI head group at *m/z* 241.0. Spectra from analysis after non-labeled fatty acid incubation were overlaid with spectra from the deuterium labeled fatty acid incubation and also with a control sample where no fatty acids were added in order to determine into which phospholipids the [D5] ALA and [D2] LA were incorporated.

Calculating the relative quantification of lipid species

To calculate the relative level of phospholipids incorporated into PC12 cell membranes, selected ions were normalized to the number of pixels per area of interest covered by the cells to subtract background signals. The signal intensities of PC species were then normalized to the peak at *m/z* 184.1 in positive mode, whereas in the negative ion mode, intensities of FA, PE and PI species were normalized to the peak at *m/z* 241.0. Because of peak overlap in the sample exposed with FA, the normalized peak intensity in FA samples was then subtracted from control peaks at the same *m/z* values to remove any interference. The relative amount of deuterated and nondeuterated phospholipids incorporated into the plasma membrane compared to control samples was calculated based on equation (1) given below.

$$\text{Relative amount} = \frac{I_{\text{normalized-FA}} - I_{\text{normalized-control}}}{I_{\text{normalized-control}}} \qquad (1)$$

Here, $I_{\text{normalized-FA}}$ is the normalized peak intensity at *m/z+5* for [D5] ALA and *m/z+2* for [D2] LA treatment, $I_{\text{normalized-control}}$ is the normalized peak intensity in control at correspond *m/z* values with FA incubation.

Results

Uptake of deuterated n-3 ALA and n-6 LA into the plasma membrane. PC12 cells were incubated with deuterated and nondeuterated ALA and LA to determine the accumulation of fatty acids into the cell membrane. The advantage of using deuterium-isotope-labeled FA is the ability to determine the FA accumulation and the incorporation into longer chain FAs, as well as to determine the relative amount of phospholipids that incorporate into the cell membrane. The images of single cells collected with the ION-TOF V demonstrate the localization of n-3 ALA and n-6 LA absorbed into the cell membrane. The

mass spectra of fatty acid species are also provided in Figure S1.

Figure 1 shows the negative ion SIMS images of control and incubated samples. The intensity of peak at m/z 277.2 is more dominant compared to the same peak in control and [D5] ALA sample (Figure 1A-C). The cells treated with [D5] ALA containing 5 deuterium atoms reveal a high intensity peak at *m/z* 282.3, whereas the same peak in the control cells or those incubated with nondeutrated ALA is low (Figure 1D-F). Similarly, we observe LA incorporation in the sample incubated with LA and [D2] LA. Figure 1H exhibits the more dominant FA (18:2) at *m/z* 279.2 peak for LA. In contrast, in the sample incubated with [D2] LA containing 2 deuterium atoms, a more intense peak at *m/z* 281.2 is observed compared to the other samples (Figure 1L). We also observe that the abundance of FA(18:1) at *m/z* 281.2 in the sample with LA treatment is higher compared to control. This is caused by an overlap between FA(18:1) and [D2] FA(18:2) with the same peak at *m/z* 281.2.

n-3 ALA and n-6 LA synthesis in the plasma membrane. In the sample incubated with [D5] ALA, the ion species with *m/z+5* represent the incorporation of phospholipids and do not overlap with any endogenous fragments in the mass spectrum. However, most of the molecules with *m/z+2* selected in the sample treated with [D2] LA overlap with other endogenous phospholipids. To confirm that the signal change after incubation is indeed from the converted fatty acids from [D2] LA, the spectrum from the nondeuterated LA treatment was also examined. The peak for the nondeuteriated fatty acid was compared with the peak two mass units higher (*m/z* +2) for the deuteriated sample. Table 1 gives assignments for the peaks incubated with labeled and non-labeled ALA and LA. All peaks analyzed, in nondeuterated and deuterated forms, are provided in Tables S1 and S2.

After incubation with ALA, the spectra obtained from the ToF-SIMS *J105* analysis in negative ion mode (Figure 2A) show increases in FAs with 20 and 22 carbons for both the n-3 ALA and the deuterium labeled n-3 ALA ([D5] ALA). The peaks at *m/z* 301.2, 303.2, 305.2, 329.3, 331.3, and 333.3 are the $[M-H]^-$ ions of FA(20:5), (20:4), (20:3), (22:5), (22:4), and (22:3), respectively, and are shown to increase in the spectrum from the samples incubated with nondeuterium labeled ALA.

For the incubation with the [D5] ALA, an increase in the same FA peaks is observed at five mass units higher due to the five deuterium labels, hence, the peaks at *m/z* 306.2, 308.2, 310.2, 334.3, 336.3, and

338.3 can be observed to increase (Figure 2A). This observed change of the deuterium labeled ALA indicates that the increase is due to conversion to the FAs followed by incorporation of the incubated ALA into the cell membrane, and not an upregulation of endogenous FAs. The well-established metabolic pathway for C18:3n-3 ALA in biological systems, gives rise to longer chain PUFAs such as C20:4, C20:5, C22:5 and C22:6 in a series of steps. This corresponds well with the observed increase in FAs in Figure 2A. However, there is no change observed in FA(22:6) in our experiments using ToF-SIMS. The FA(22:6) is the end product in the fatty acid synthesis pathway. Thus, the amount of FA(22:6) created from conversion of the incubated ALA is apparently too small to be able to observe any significant differences between control and ALA incubated samples (26).

The same trends are observed in Figure 2B for incubation with linoleic acid (LA, C18:2n-6), where LA is readily converted into longer-chain PUFAs including FA(20:4), FA(20:3), FA(20:2), and FA(20:1). The increase in these PUFAs is detected for both incubation with non-labeled LA and [D2] LA, the same observation as for the ALA incubated samples. However, there is no significant increase in the long-chain conversion of fatty acids with 22 carbons. Our finding is consistent with the synthesis pathway of n-6 LA where LA is mostly converted into low long-chain FA with 20 carbons, in human and animal models (1, 27, 28). The observed increase in specific FAs for the LA and [D2] LA incubation matches well with the metabolic pathway for LA in biological systems, where it is converted to C18:3, C20:3, C20:4, C22:4 and C22:5.

Incorporation of ALA and LA into plasma phospholipids. PC12 cells internalize the supplemental n-3 and n-6 fatty acids and proceed to the metabolic conversion and incorporation of the FAs into the phospholipids in the cell membrane (1). To identify the incorporation of the n-3 ALA and n-6 LA into the cell membrane, the mass spectra of control, deuterated- and nondeuterated-treated samples have been compared to track the deuterium labels on the fatty acids used for incubation. The ion dose was kept below the static limit in order to confirm that the analyzed species originates from the cell membrane and not from the cytoplasm. As mentioned above, the peaks at *m/z+5* and *m/z+2* in cells incubated with [D5] ALA and [D2] LA, respectively, were chosen and then confirmed with the

nondeuterated forms of the same species.

Figure 3 shows the conversion and incorporation of ALA and [D5] ALA into phospholipids. For example, in negative ion mode, we found that the peak for the species PE(36:3), PE(38:3), PE(38:4), PE (38:5), PI(36:3), and PI(38:5) were increased in the spectra after incubation with ALA or the [D5] ALA indicating an incorporation of ALA into this species (Figure 3B).

Figure 4 reveals the incorporation of LA into phospholipids where an increase can be seen for different species. For example the signal intensities of species PE(36:2), PI(38:2), PI(38:2) and PI(38:4) observed in negative ion mode give higher signal intensity in FA-incubated samples compared to control (Figure 4B). Table 1 provides a complete list of the phospholipid peaks that were found changing after incubation for both the ALA and LA incubation (with and without the deuterium label). In general, the synthesis of PCs, PEs, and PIs use ALA for incorporation into lipids with 3, 5, and 6 double bonds whereas the LA incorporates into phospholipids with 2 and 4 double bonds.

Comparison of the incorporation levels for ALA and LA into cellular phospholipids. The peaks at *m/z* 184.1 and 241.0 are head group fragment ions of PC and PI, respectively, and we use these as the membrane standard. To calculate the level of incorporation, we assumed that the total amount of endogenous phospholipids stays unchanged. Therefore, the intensity of PC and PI head group fragments is approximately similar or only slightly altered in all the samples. The change in signal following both the nondeuterated LA and the deuterated treatment is then used to establish the amount of phospholipid turnover. The level of incorporation was calculated for both treatments and compared to each other.

To identify the phospholipid turnover and their relative amounts, both nondeuterated and deuterated FAs were exposed to the cells. The nondeuterated FA incubation was used for comparison with the enrichment caused from deuterium-isotopic labeled fatty acids. The relative level of FA and phospholipid incorporation into plasma membrane was calculated using the intensity ratio between control and treated-samples (Equation 1).

As expected, an increased amount of ALA and LA is found in PC12 cell membranes in treated-samples (Figure S2). Interestingly, the accumulation of ALA is ~50% higher than LA in the cell membrane

($p<0.05$, *Student's t test*) even when their incubation concentrations in the experiments are the same. In the treated samples, the incorporation level of ALA increases 2 times compared to a 150% increase for LA when compared to controls. We also obtained the relative amount of long chain PUFAs converted from those FAs. Most of the FA species, such as FA(20:5), FA(20:4), FA(20:3), FA(22:5), and FA(22:4), biosynthesized from ALA are from the range 100% to 150% higher than the level observed in control cells. Our data are supported by Hussein *et al.* using [13C] ALA and LA. They also found an over 3-fold increase in ALA, and 2-fold increase in FA(20:5) and (22:5) in erythrocyte membranes in human blood samples when incubated with lipids (37). In contrast, a smaller increase in FA(22:3), about 50%, is found in the ALA-treated sample. Similarly, we obtained an increase in metabolites of LA in the LA-exposed sample. For example, FA(20:4) and FA(20:1) increase approximately 50% whereas FA(20:3) and FA(20:2) is approximately doubled compared to control.

Figure 5 shows the increase in the relative amount of phospholipids after incubation with ALA and [D5] ALA compared to control (~100%, Table S3). In the positive ion mode, the amount of PC turnover is increased about 60%. Likewise, PE species in treated samples, such as PE(38:5), PE(38:4), and PE(38:3), are found to be in a range from 50% to 70% increased compared to control; except PE(36:3), which is about 90% higher. However, the amount of PE turnover is about half the level of incorporated PI in ALA-treated samples. For example, a 110% increase in PI(36:3) and PI(38:5) is found. Consistent with our results, others have shown similar amounts of incorporation of ALA and its converted PUFAs into PCs and PEs in human Y79 retinoblastoma cells (38).

The comparison between the relative amount of phospholipid turnover from LA and [D2] LA was examined to confirm the actual amount of incorporated phospholipids into cell membranes and to rule out incorporation from other endogenous lipids. Figure 6 shows the increase in relative amount of phospholipids after incubation with LA and [D2] LA compared to control (~100%, Table S4). Cells incubated with LA have a phospholipid turnover that is significantly increased compared to non-treated control cells. The amount of PCs synthesized by LA and its converted PUFAs are approximately 40-50% higher than non-treated samples. Almost 100% of PE and PI levels, especially PE(36:2) and PI(36:2), are increased in LA-incubated cells, whereas an increase of about a 60% in PE (38:2) and PI(38:4) is observed. Overall, the amount of total phospholipids incorporated from LA is ~40% less than

those from ALA although the same concentrations of ALA and LA are used for incubation ($p<0.05$). This finding is correlated with the amount of FAs incorporated in the cell membrane and shown in Figure S2.

Discussion

Understanding the lipid metabolism are important to gain more knowledge about cell functions. Therefore, using stable isotopic-labeled tracers, we were able to track the incorporation of the essential fatty acids into other fatty acid products as well as the incorporation into phospholipids. The stable isotopic-labeled tracers also make it possible to determine the relative quantitative information of incorporated products in the plasma membrane, providing new insights into membrane lipid metabolism. Herein, we introduce a method to visualize and relatively quantify phospholipids in PC12 cell membrane. ToF-SIMS analysis with two instruments, one using a LMIG and the other a GCIB, provides spatial information about the incorporated fatty acids as well as the ability to detect intact lipid species.

The n-3 and n-6 FAs cannot be synthesized by the cell and therefor need to be provided by an exogenous (dietary) source. Accumulation of both n-3 and n-6 fatty acids in cellular membranes and tissues has been shown in previous studies (29, 30), indicating that the essential fatty acids are of particular importance to maintain critical functions for the cell and are therefore important for the cell to store in the form of various phospholipids in, for example, cellular membranes. In this experiment, ToF-SIMS shows that the increased level of ALA and LA observed after incubation suggests a high uptake of both the FAs into the cell from the surrounding media. Additionally, the results from incubation with deuterium labeled FAs reveal that the formation of converted PUFAs from ALA and LA are different. Only PUFAs with 20 carbons are produced from LA, while ALA can convert into PUFAs with both 20 and 22 carbons. Also, our data suggest that ALA (with 3 double bonds) or its conversion product EPA C20:5 (with 5 double bonds), is incorporated without further addition of double bonds, in either one or both fatty acid positions in the phospholipid, creating lipid molecules with 3, 5 or 6 double bonds. The

same is true for LA (with 2 double bonds) and the conversion product AA (with 4 double bonds), which might be incorporated into phospholipids to create lipids with 2 and 4 double bonds.

Importantly, various unsaturated phospholipids generated originated from ALA and LA in the cell membrane. The data further indicate that the ALA and LA are converted and incorporated into a range of lipid species such as, PC, PE, and PI, see Figure 3 and 4 and Table 1. The selectivity of incorporation of PUFAs into phospholipids has been previously investigated where incorporation in PC and PE were found (31, 32). It has also been shown that ALA is converted to DHA in developing rat brain,[33] and can thereafter be incorporated into specific phospholipids such as PC, PE and PI *in vivo* (34). The same is true in studies of cells, where Li *et al.* and Stulnig *et. al* reported that T cells incubated with EPA, 20:5n-3, which is part of the metabolic pathway for ALA, show altered lipid membrane composition, where enrichment is observed in the PE species substituted with 36:5, 36:5, 38:6, 38:5, 40:7, 40:6, 40:5 acyl chains, PI species substituted with 36:4, 36:1, 38:5, 40:6, 40:5 acyl chains, and PC species substituted with 36:3, 36:4, 38:6, 38:5 and 40:6 acyl chains (35, 36). The results from these previous studies are in good agreement with the differences in cell membrane composition observed between the control cells and the ALA- or LA-incubated cells, where these are incorporated into PC, PE and PI.

Based on ToF-SIMS data, the relative amounts of phospholipid turnover generated originated from ALA and LA in plasma membrane was calculated using the intensity ratio between control and treated-samples. We find that the accumulated amount of ALA and its converted PUFAs is more than that of LA and its long chain PUFAs. From those results, we suggest that the relative levels of phospholipids synthesized by LA is less than by ALA. This is an important finding as unsaturated phospholipids incorporated into the cell membrane can alter the physical properties of the membrane, such as flexibility and solubility, which promotes the membrane fluidity. Moreover, the flexible unsaturated PUFAs also stimulate the formation of the SNARE complex in vesicle fusion that plays an important role in exocytosis (39). It is well known that consumption of n-3 and n-6 FAs can change the plasma membrane lipid compositions, which in turn can reduce the risk of mental disorders (40). Hence, our findings are

important results for understanding which specific phospholipids might be involved in the neurodegenerative diseases and suggest a basic pathway for protection against unhealthy brain aging.

Acknowledgments

The mass spectrometry analysis were performed at Go:IMS in Gothenburg. We thank Dr. John Fletcher for his help regarding instrumental issues with the *J105*. This study was supported by the Knut and Alice Wallenberg Foundation, the USA National Institutes of Health, European Research Council (ERC) and the Swedish Research Council.

References

1. Emken, E. A., R. O. Adlof, H. Rakoff, W. K. Rohwedder and R. M. Gulley. 1990. Metabolism in vivo of deuterium-labelled linolenic and linoleic acids in humans. *Biochem Soc Trans* **18: 766-9**.
2. Wall, R., R. P. Ross, G. F. Fitzgerald and C. Stanton. 2010. Fatty acids from fish: the anti-inflammatory potential of long-chain omega-3 fatty acids. *Nutr Rev* **68: 280-9**.
3. Weiser, M. J., C. M. Butt and M. H. Mohajeri. 2016. Docosahexaenoic Acid and Cognition throughout the Lifespan. *Nutrients* **8: 99**.
4. Calder, P. C. 2009. Polyunsaturated fatty acids and inflammatory processes: New twists in an old tale. *Biochimie* **91: 791-5**.
5. Corsinovi, L., F. Biasi, G. Poli, G. Leonarduzzi and G. Isaia. 2011. Dietary lipids and their oxidized products in Alzheimer's disease. *Mol Nutr Food Res* **55 Suppl 2: S161-72**.
6. Khandelwal, S., L. Kelly, R. Malik, D. Prabhakaran and S. Reddy. 2013. Impact of omega-6 fatty acids on cardiovascular outcomes: A review. *J Preventive Cardiol* **2: 325-336**.
7. Parletta, N., T. Niyonsenga and J. Duff. 2016. Omega-3 and Omega-6 Polyunsaturated Fatty Acid Levels and Correlations with Symptoms in Children with Attention Deficit Hyperactivity Disorder, Autistic Spectrum Disorder and Typically Developing Controls. *PLoS One* **11: e0156432**.
8. Kidd, P. M. 2007. Omega-3 DHA and EPA for cognition, behavior, and mood: clinical findings and structural-functional synergies with cell membrane phospholipids. *Altern Med Rev* **12: 207-27**.
9. Schaefer, E. J., V. Bongard, A. S. Beiser, S. Lamon-Fava, S. J. Robins, R. Au, K. L. Tucker, D. J. Kyle, P. W. Wilson and P. A. Wolf. 2006. Plasma phosphatidylcholine docosahexaenoic acid content and risk of dementia and Alzheimer disease: the Framingham Heart Study. *Arch Neurol* **63: 1545-50**.
10. Jump, D. B., C. M. Depner and S. Tripathy. 2012. Omega-3 fatty acid supplementation and cardiovascular disease. *J Lipid Res* **53: 2525-45**.
11. Bos, D. J., B. Oranje, E. S. Veerhoek, R. M. Van Diepen, J. M. Weusten, H. Demmelmair, B. Koletzko, M. G. de Sain-van der Velden, A. Eilander, M. Hoeksma and S. Durston. 2015. Reduced Symptoms of Inattention after Dietary Omega-3 Fatty Acid Supplementation in Boys with and without Attention Deficit/Hyperactivity Disorder. *Neuropsychopharmacology* **40: 2298-306**.
12. Delpech, J. C., C. Madore, C. Joffre, A. Aubert, J. X. Kang, A. Nadjar and S. Laye. 2015. Transgenic increase in n-3/n-6 fatty acid ratio protects against cognitive deficits induced by an immune challenge through decrease of neuroinflammation. *Neuropsychopharmacology* **40: 525-36**.
13. Molfino, A., G. Gioia, F. Rossi Fanelli and M. Muscaritoli. 2014. The role for dietary omega-3 fatty acids supplementation in older adults. *Nutrients* **6: 4058-73**.
14. Dangour, A. D., V. A. Andreeva, E. Sydenham and R. Uauy. 2012. Omega 3 fatty acids and cognitive health in older people. *Br J Nutr* **107 Suppl 2: S152-8**.
15. Marszalek, J. R., C. Kitidis, A. Dararutana and H. F. Lodish. 2004. Acyl-CoA synthetase 2 overexpression enhances fatty acid internalization and neurite outgrowth. *J Biol Chem* **279: 23882-91**.
16. Darios, F. and B. Davletov. 2006. Omega-3 and omega-6 fatty acids stimulate cell membrane expansion by acting on syntaxin 3. *Nature* **440: 813-7**.

17. Ikeda, I., K. Mitsui and K. Imaizumi. 1996. Effect of dietary linoleic, alpha-linolenic and arachidonic acids on lipid metabolism, tissue fatty acid composition and eicosanoid production in rats. *J Nutr Sci Vitaminol (Tokyo)* **42: 541-51**.
18. Hoene, M., J. Li, H. U. Haring, C. Weigert, G. Xu and R. Lehmann. 2014. The lipid profile of brown adipose tissue is sex-specific in mice. *Biochim Biophys Acta* **1842: 1563-70**.
19. Malmberg, P., E. Jennische, D. Nilsson and H. Nygren. 2011. High-resolution, imaging TOF-SIMS: novel applications in medical research. *Anal Bioanal Chem* **399: 2711-8**.
20. Cheng, J., J. Kozole, R. Hengstebeck and N. Winograd. 2007. Direct Comparison of Au_3^+ and C_{60}^+ Cluster Projectiles in SIMS Molecular Depth Profiling. *Journal of the American Society for Mass Spectrometry* **18: 406-412**.
21. Richter, K., H. Nygren, P. Malmberg and B. Hagenhoff. 2007. Localization of fatty acids with selective chain length by imaging time-of-flight secondary ion mass spectrometry. *Microsc Res Tech* **70: 640-7**.
22. Angerer, T. B., P. Blenkinsopp and J. S. Fletcher. 2015. High energy gas cluster ions fororganic and biological analysis by time-of-flight secondary ion massspectrometry. *International Journal of Mass Spectrometry* **377: 591-598**.
23. Fletcher, J. S., S. Rabbani, A. M. Barber, N. P. Lockyer and J. C. Vickerman. 2013. Comparisonof C-60 and GCIB primary ion beams for the analysis of cancer cells andtumour sections. *Surf. Interface Anal.* **45: 273-276**.
24. Fletcher, J. S., S. Rabbani, A. Henderson, P. Blenkinsopp, S. P. Thompson, N. P. Lockyer and J. C. Vickerman. 2008. A New Dynamic in Mass Spectral Imaging of Single Biological Cells. *Analytical Chemistry* **80: 9058-9064**.
25. Hill, R., P. Blenkinsopp, S. Thompson, J. Vickerman and J. S. Fletcher. 2011. A new time-of-flight SIMS instrument for 3D imaging and analysis. *Surface and Interface Analysis* **43: 506-509**.
26. Pawlosky, R. J., J. R. Hibbeln, J. A. Novotny and N. Salem, Jr. 2001. Physiological compartmental analysis of alpha-linolenic acid metabolism in adult humans. *J Lipid Res* **42: 1257-65**.
27. Demmelmair, H., B. Iser, A. Rauh-Pfeiffer and B. Koletzko. 1999. Comparison of bolus versus fractionated oral applications of [13C]-linoleic acid in humans. *Eur J Clin Invest* **29: 603-9**.
28. Su, H. M., T. N. Corso, P. W. Nathanielsz and J. T. Brenna. 1999. Linoleic acid kinetics and conversion to arachidonic acid in the pregnant and fetal baboon. *J Lipid Res* **40: 1304-12**.
29. Healy, D., F. Wallace, E. Miles, P. Calder and P. Newsholme. 2000. Effect of low-to-moderate amounts of dietary fish oil on neutrophil lipid composition and function. *Lipids* **35: 763-768**.
30. Bazan, N. and B. Scott. 1990. Dietary omega-3 fatty acids and accumulation of docosahexaenoic acid in rod photoreceptor cells of the retina and at synapses. *Upsala journal of medical sciences. Supplement* **48: 97-107**.
31. Masui, H., R. Urade and M. Kito. 1997. Selective incorporation of polyunsaturated fatty acids into organelle phospholipids of animal cells. *Bioscience, biotechnology, and biochemistry* **61: 900-902**.
32. Lands, W., M. Inoue, Y. Sugiura and H. Okuyama. 1982. Selective incorporation of polyunsaturated fatty acids into phosphatidylcholine by rat liver microsomes. *Journal of Biological Chemistry* **257: 14968-14972**.
33. Dhopeshwarkar, G. A. and C. Subramanian. 1976. Biosynthesis of polyunsaturated fatty acids in the developing brain: I. Metabolic transformations of intracranially administered 1-14C linolenic acid. *Lipids* **11: 67-71**.
34. Green, P. and E. Yavin. 1993. Elongation, desaturation, and esterification of essential fatty acids by fetal rat brain in vivo. *Journal of lipid research* **34: 2099-2107**.
35. Li, Q., L. Tan, C. Wang, N. Li, Y. Li, G. Xu and J. Li. 2006. Polyunsaturated eicosapentaenoic acid changes lipid composition in lipid rafts. *European journal of nutrition* **45: 144-151**.
36. Stulnig, T. M., J. Huber, N. Leitinger, E.-M. Imre, P. Angelisová, P. Nowotny and W. Waldhäusl. 2001. Polyunsaturated eicosapentaenoic acid displaces proteins from membrane rafts by altering raft lipid composition. *Journal of Biological Chemistry* **276: 37335-37340**.
37. Hussein, N., E. Ah-Sing, P. Wilkinson, C. Leach, B. A. Griffin and D. J. Millward. 2005. Long-chain conversion of [13C]linoleic acid and alpha-linolenic acid in response to marked changes in their dietary intake in men. *J Lipid Res* **46: 269-80**.

38. Goustard-Langelier, B., J. M. Alessandri, G. Raguenez, G. Durand and Y. Courtois. 2000. Phospholipid incorporation and metabolic conversion of n-3 polyunsaturated fatty acids in the Y79 retinoblastoma cell line. *J Neurosci Res* **60: 678-85**.
39. Darios, F., E. Connell and B. Davletov. 2007. Phospholipases and fatty acid signalling in exocytosis. *J Physiol* **585: 699-704**.
40. Cole, G. M., Q. L. Ma and S. A. Frautschy. 2010. Dietary fatty acids and the aging brain. *Nutr Rev* **68 Suppl 2: S102-11**.

Table 1: Assignment for selected peaks for samples incubated with deuteriated and nondeuteriated ALA and LA

	Nondeuterated ALA		[D5] ALA		Nondeuterated LA		[D2] LA	
	Measured m/z	Assignment	Measured m/z	Assignment	Measured m/z	Assignment	Measured m/z	Assignment
Positive ion mode $[M+H]^+$ unless specified +Na/K	760.6	PC (34:1)	765.6	[D5] PC(34:1)	758.6	PC(34:2)	760.6	[D2] PC(34:2)
	794.5	PC(34:3)+K	799.5	[D5] PC(34:3)+K	786.6	PC(36:2)	788.6	[D2] PC(36:2)
	806.6	PC(38:6)	811.6	[D5] PC(38:6)	808.6	PC(36:2)+Na	810.6	[D2] PC(36:2)+Na
	808.6	PC (38:5)	813.6	[D5] PC(38:5)	824.6	PC(36:2)+K	826.6	[D2] PC(36:2)+K
	818.5	PC(36:5)+K	823.5	[D5] PC(36:5)+K	852.6	PC(38:2)+K	854.6	[D2] PC(38:2)+K
	820.5	PC(36:4)+K	825.5	[D5] PC(36:4)+K				
	822.5	PC(36:3)+K	827.5	[D5] PC(36:3)+K				
Negative ion mode $[M-H]^-$	740.5	PE(36:3)	745.5	[D5] PE(36:3)	742.5	PE(36:2)	744.5	[D2] PE(36:2)
	764.5	PE(38:5)	769.5	[D5] PE(38:5)	770.6	PE(38:2)	772.6	[D2] PE(38:2)
	766.5	PE(38:4)	771.5	[D5] PE(38:4)	861.6	PI(36:2)	863.6	[D2] PI(36:2)
	768.6	PE(38:3)	773.6	[D5] PE(38:3)	885.6	PI(38:4)	887.6	[D2] PI(38:4)
	859.5	PI(36:3)	864.5	[D5] PI(36:3)				
	883.5	PI(38:5)	888.5	[D5] PI(38:5)				

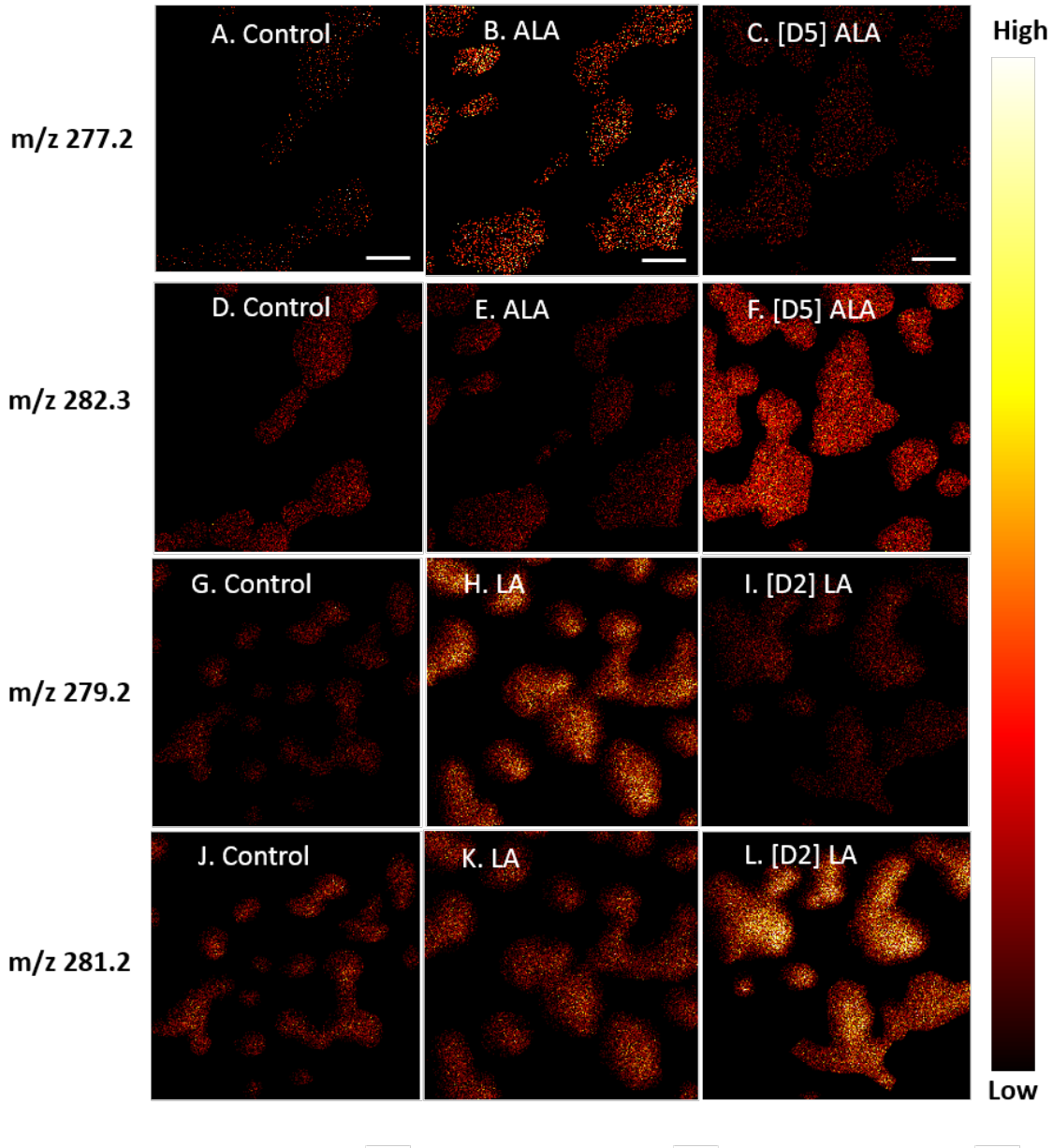

Figure 1. ToF-SIMS ion images show accumulation of fatty acids into cell membrane using the *ION-TOF V* equipped with a 25 keV Bi_3^{++} LMIG in negative ion mode. (A) Control, (B) ALA-treated cells, (C) [D5] ALA-treated cells at *m/z* 277.2; (D) Control, (E) ALA-treated cells, (F) [D5] ALA-treated cells at *m/z* 282.3; (G) control, (H) LA-treated cells, (I) [D2] LA-treated cells at *m/z* 279.2; (J) control, (K) LA-incubated cells, (L) [D2] LA-incubated cells at *m/z* 281.2. Image area is 255 x 255 μm^2 and 256 x 256 pixel. Scale bar is 40 µm.

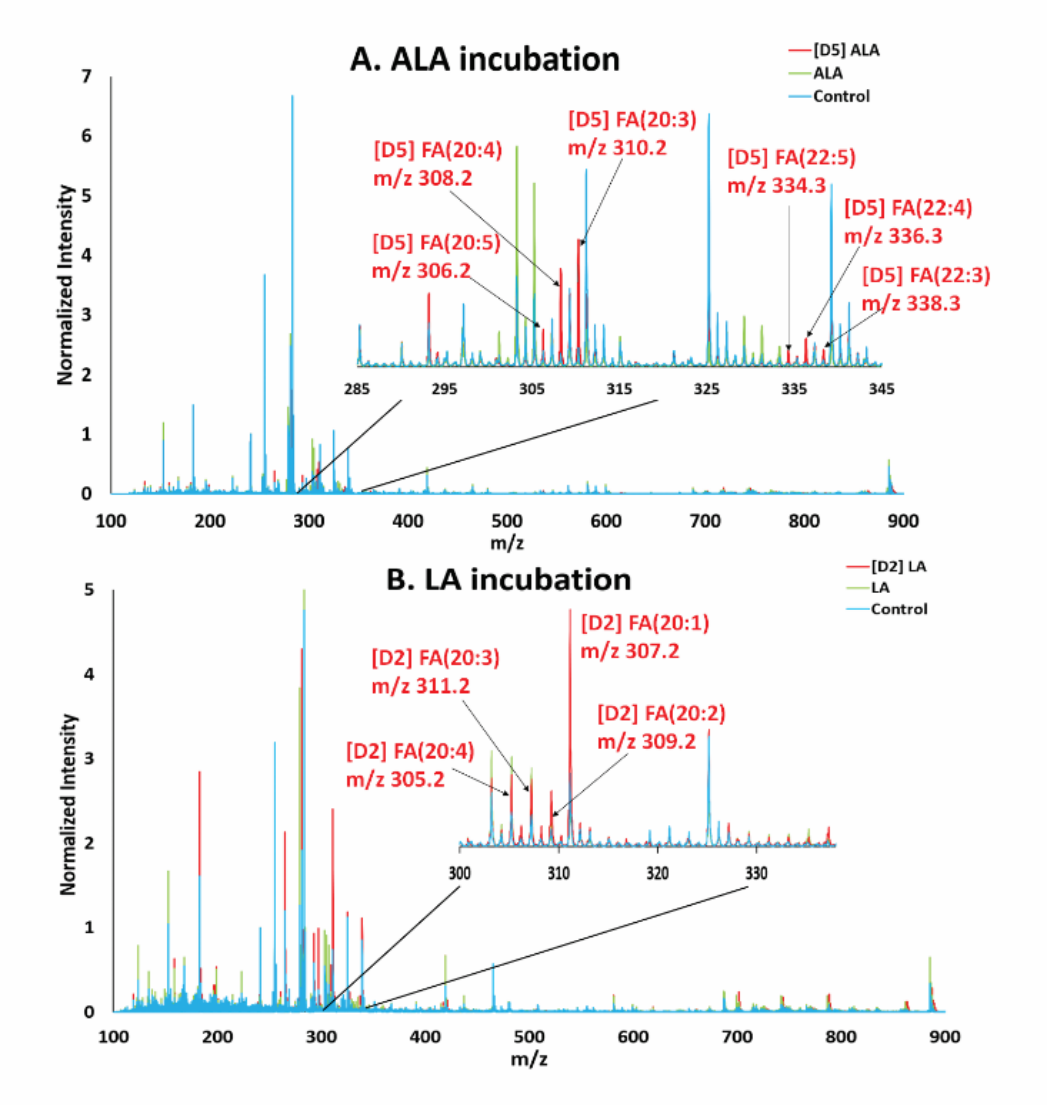

Figure 2. Overlayed spectra of converted fatty acids from incubation with (A) ALA and [D5] ALA; (B) LA and [D2] LA analyzed using *J105*/40 keV $(CO_2)_{6000}^+$ GCIB (negative ions). Peak intensity is normalized to number of pixels selected and PI fragment at *m/z* 241.0.

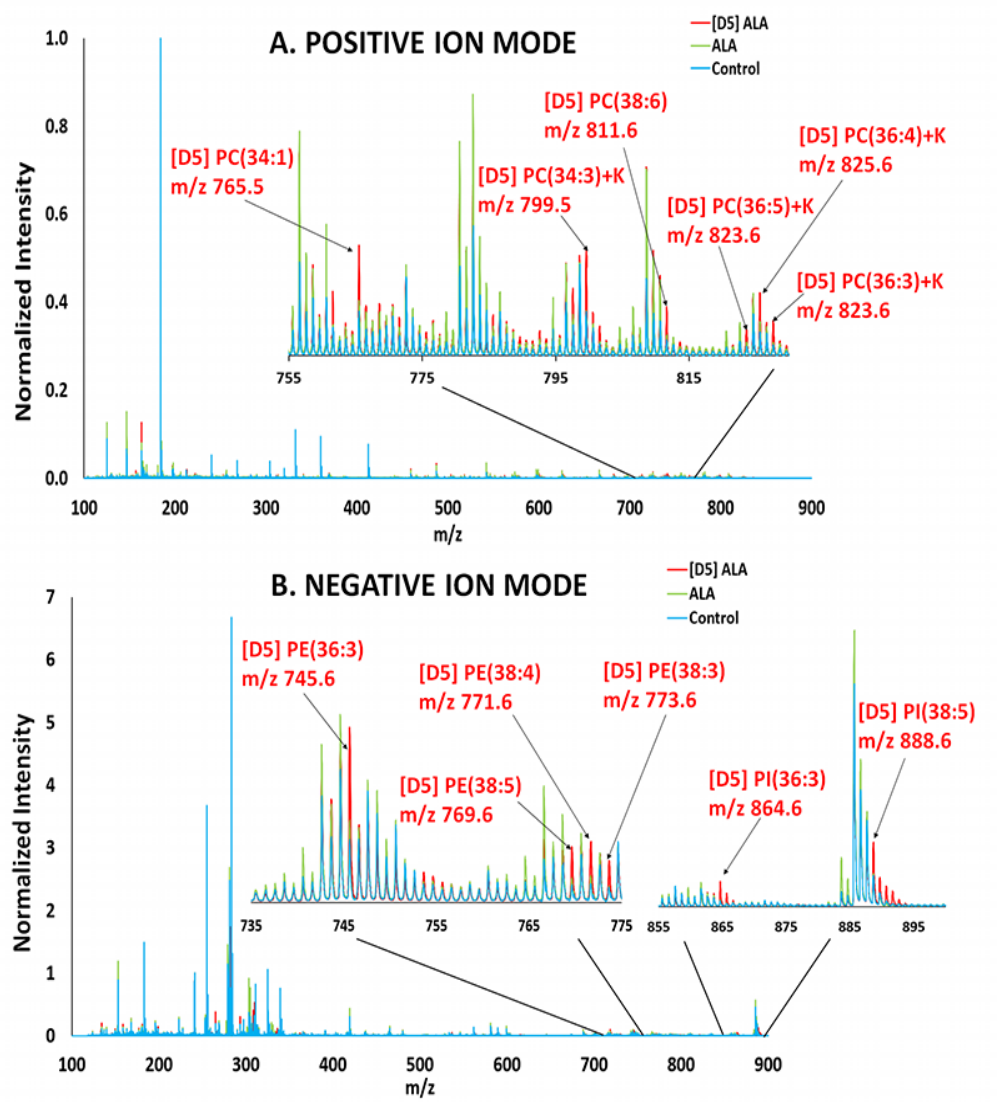

Figure 3. Phospholipid turnover from ALA and [D5] ALA in (A) positive ion mode, (B) negative ion mode analyzed using *J105*/40 keV $(CO_2)_{6000}^+$ GCIB. Peak intensity is normalized to number of pixels selected and PC fragment at *m/z* 184.1 (positive mode) or PI fragment at *m/z* 241.0 (negative mode). PCs are detected as $[M+H]^+$ ions unless specified as +K. PEs and PIs are detected as $[M-H]^-$.

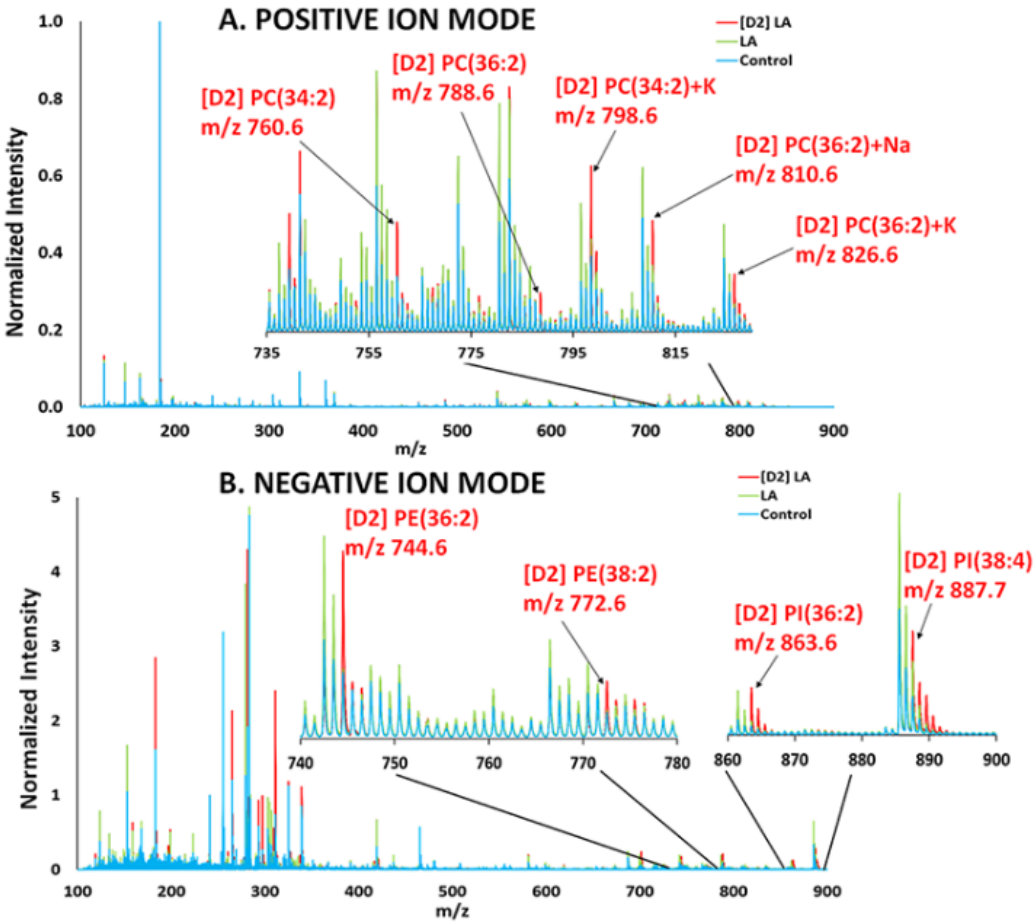

Figure 4. Phospholipid turnover from LA and [D2] LA in (A) positive ion mode, (B) negative ion mode analyzed using *J105*/40 keV $(CO_2)_{6000}^+$ GCIB. Peak intensity is normalized to number of pixels selected and PC fragment at *m/z* 184.1 (positive mode) or PI fragment at *m/z* 241.0 (negative mode). PCs are detected as $[M+H]^+$ ions unless specified as +K or +Na. PEs and PIs are detected as $[M-H]^-$.

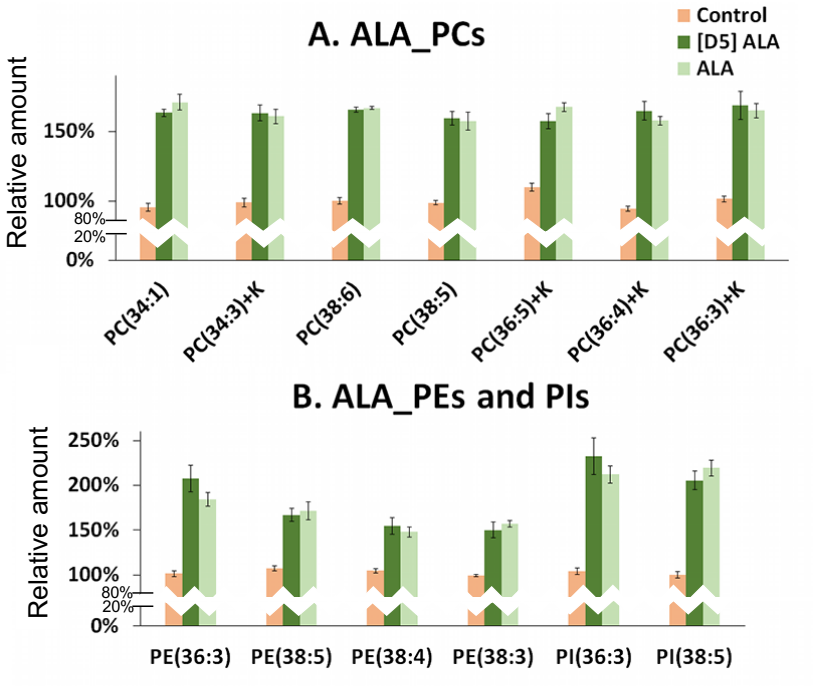

Figure 5. The relative amount of phospholipids after incubation with ALA and [D5] ALA for (A) PC molecules in positive ion mode; (B) PE and PI species in negative ion mode analyzed using *J105*/40 keV $(CO_2)_{6000}^+$ GCIB. The increase is calculated by comparing to control samples. Peak intensity is normalized to number of pixels selected and the PC head group at *m/z* 184.1 for positive ion mode or the PI fragment at *m/z* 241.0 for negative ion mode. The error bar shows standard error of mean. The relative levels of phospholipids are calculated for 3 cell generations (n=3).

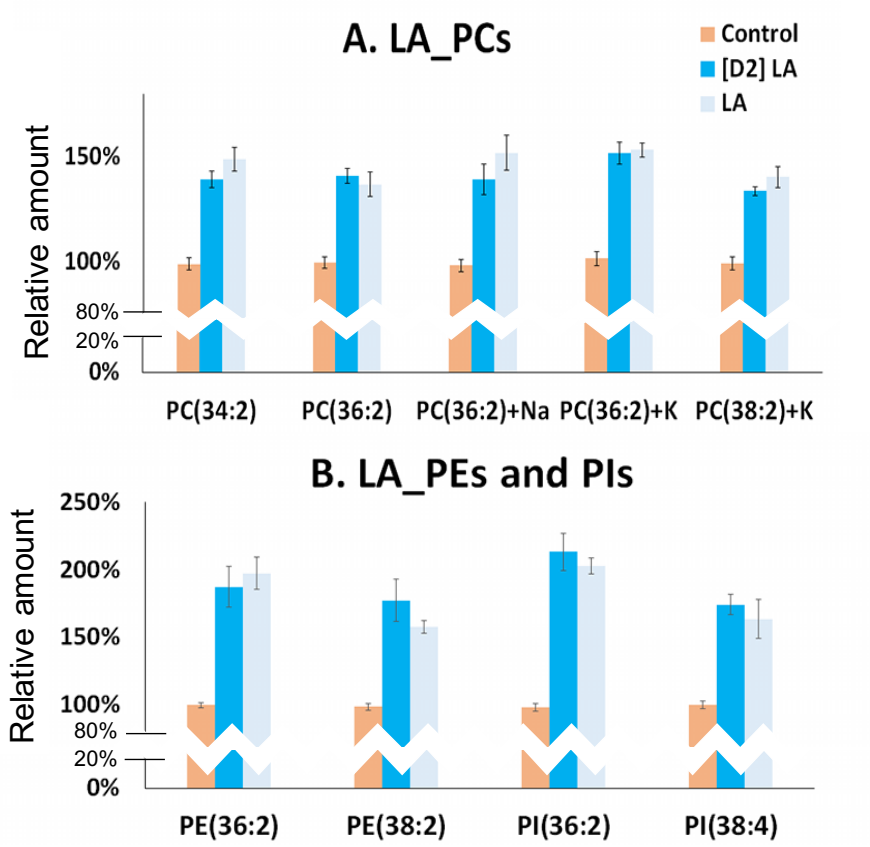

Figure 6. The relative amount of phospholipids after incubation with LA and [D2] LA for (A) PC species in positive mode; (B) PE and PI species in negative ion mode analyzed using *J105*/40 keV $(CO_2)_{6000}^+$ GCIB. The increase is calculated by comparing to control samples. Peak intensity is normalized to number of pixels selected and the PC head group at *m/z* 184.1 for positive ion mode or the PI fragment at *m/z* 241.0 for negative ion mode. The error bars are standard error of mean. The relative levels of phospholipids are calculated for 3 cell generations (n=3).